Theory of Air-Coupled Flexural Waves

Frank Press and Maurice Ewing

Theory of Air-Coupled Flexural Waves*

Frank Press and Maurice Ewing†

Lamont Geological Observatory, Columbia University, Palisades, New York

(Received December 26, 1950)

The theory of air-coupled flexural waves in a floating ice sheet is derived for the case of an impulsive point source situated either in the air or in the water. It is found that new branches are introduced to the dispersion curve of flexural waves as a result of coupling to compressional waves in the atmosphere. Experimental data are briefly reviewed.

INTRODUCTION

IN the course of a study of the phenomena associated with the famous explosion of the volcano Krakatoa[1,2] in the Straits of Sunda, the authors noted a simultaneous arrival of an air wave and tidal disturbance at several widely separated locations. While this curious phenomenon was noticed previously,[3] it had been passed off as a coincidence, with the tidal waves attributed to non-related earthquakes. It is now our belief that the simultaneous arrival of an air wave and tidal disturbance resulted from coupling between the atmospheric pressure wave and the ocean.

It is surprising at first to think of coupling between the atmosphere and the ocean, especially since the density contrast between the two media is so great. It can generally be shown, however, that coupling between air waves and surface waves of all types is appreciable when the phase velocity of the surface wave is very close to the speed of sound in air. To a first approximation the reaction of the surface wave on the air can be neglected and the air wave can be treated simply as a pressure pulse travelling over the surface of a dispersive system. Following Lamb's method,[4–6] the effect of a travelling disturbance can be obtained by the application of a succession of infinitesimal impulses at equal intervals of time, each impulse producing a dispersive system of waves. Superposition of the wave systems of the successive impulses results in reinforcement only for those waves (having one or more discrete frequencies) whose phase velocity equals the velocity component of the travelling disturbance in the direction of wave propagation. Since waves associated with a given frequency are propagated with the group velocity, the wave system generated by a travelling disturbance either precedes or follows the disturbance according to whether the group velocity is greater than or less than the phase velocity. Air coupled flexural waves illustrate the first case in which the coupled waves precede the air pulse. Hydrodynamic gravity waves in very deep water would follow the arrival of the air pulse. Possible existence of air coupled Rayleigh waves was discussed briefly by Bateman.[7]

Since the coupling to air is loose, the frequency of an air-coupled surface wave may be obtained in a simple fashion by equating the velocity of sound in air to the phase velocity for the particular type of surface wave being considered, using the characteristic equation for the surface wave in the form which ignores the influence of the air.

The existence of air-coupled surface waves was firmly established in a series of experiments performed on floating ice sheets in Lake Superior and Lake Cayuga.[8] Although these experiments were organized for another purpose, coupling between air waves and flexural waves of the ice sheet was recognized and studied under controlled conditions.

In this paper a more complete theory for air-coupled flexural waves in a floating ice sheet is derived for the case of an impulsive point source situated either in the air or in the water beneath the ice. Sufficient experimental results are given for a comparison with theory to be made.

A complete discussion of the theory of air-coupled gravity waves, with application to the explosion of Krakatoa, is reserved for another paper. An analogous theory for air-coupled Rayleigh waves will be submitted for publication shortly.

THE THEORY

Consider the propagation of flexural waves in a plate of infinite extent floating on deep water, the thickness of the plate H being small compared to wavelengths considered. Overlying the plate is an infinite atmosphere having density ρ_1, and sound velocity v_1. The plate has volume density ρ_2, longitudinal wave velocity v_p; the water has density ρ_3, sound velocity v_3, A cartesian coordinate system is chosen with the x, y axes in the equilibrium plane of the plate and the z axis vertically upward. We will use the coordinates z and $r = (x^2 + y^2)^{\frac{1}{2}}$

[1] G. J. Symond, *The Eruption of Krakatoa and Subsequent Phenomena* (Trubner and Company, London, 1888).
[2] C. L. Pekeris, Proc. Roy. Soc. (London) **A171**, 434 (1939).
[3] R. D. M. Verbeek, Krakatau, Batavia (1886).
[4] H. Lamb, Phil. Mag. **31**, 387 (1916).
[5] H. Lamb, Phil. Mag. **31**, 539 (1916).
[6] H. Lamb, *Hydrodynamics* (Cambridge University Press, Teddington, England, 1932), sixth edition, pp. 413–415.

[7] H. Bateman, Proc. Natl. Acad. Sci. U. S. **24**, 315–320 (1938).
[8] Press, Crary, Oliver, and Katz, Trans. Am. Geophys. Union (to be published).

and denote the corresponding displacements by w and q. The subscripts 1, 2, 3 hereafter refer to the air, plate, and water, respectively.

Simple Harmonic Point Source in Air

We wish to determine the vertical displacement w of the plate due to the passage of a system of flexural waves which originate in a point source of sound waves at $r=0$ and $z=d$. Particular interest is in the solutions which predominate at large distances from the source. Assuming simple harmonic motion $\exp(-i\omega t)$, we introduce the velocity potentials ϕ_1 and ϕ_3 from which the component velocities $\dot{q}$ and $\dot{w}$ and the pressure p can be obtained as follows,

$$\left.\begin{array}{l} p_i = \rho_i \partial\phi_i/\partial t, \\ q_i = \partial\phi_i/\partial r, \qquad i=1,3 \\ \dot{w}_i = \partial\phi_i/\partial z. \end{array}\right\} \qquad (1)$$

It is convenient to divide the air into two regions by the plane $z=d$ and to denote values of velocity potential etc., for the region $0<z<d$ by primed symbols.

It is required that the functions ϕ be solutions of the wave equation,

$$v_i^2 \nabla^2 \phi_i = \partial^2\phi_i/\partial t^2, \quad i=1,3, \qquad (2)$$

where

$$\nabla^2 = \partial^2/\partial r^2 + (1/r)\partial/\partial r + \partial^2/\partial z^2.$$

Solutions of Eq. (2) must satisfy the boundary conditions (for a thin plate),

$$\partial\phi_1'/\partial z = \partial w_2/\partial t = \partial\phi_3/\partial z \quad \text{at} \quad z=0, \qquad (3)$$

and w_2 satisfies the equation for flexural vibrations of the plate[9]

$$H\rho_2\partial^2 w_2/\partial t^2 = -(H^3\rho_2 v_p^2/12)\nabla^4 w_2 \\ -\rho_3 g w_2 - \rho_3\partial\phi_3/\partial t + \rho_1\partial\phi_1'/\partial t, \qquad (4)$$

where v_p is the velocity of longitudinal waves in the plate, g is the gravitational acceleration, and

$$\nabla^4 = \frac{1}{r}\frac{\partial}{\partial r}\left\{r\frac{\partial}{\partial r}\left[\frac{1}{r}\frac{\partial}{\partial r}\left(r\frac{\partial}{\partial r}\right)\right]\right\}.$$

Equation (4) is derived under the assumption that Poisson's constant for the plate has the value 0.25.

We use a method of representing a simple harmonic point source originally given by Lamb.[10] The procedure is first to obtain the solutions to the problem where a periodic pressure is applied to the entire plane $z=d$ symmetrically about the z axis and then to pass to the case of a point source utilizing the fourier-bessel integral. A point source located at $r=0$, $z=d$ is represented by ultimately requiring continuity of pressure in the plane $z=d$ and continuity of vertical velocity everywhere in the same plane, except at the source where the

[9] Maurice Ewing and A. P. Crary, Physics **5**, Pt. II, No. 6, 1–10 (1934).
[10] H. Lamb, Phil. Trans. Roy. Soc. (London) **A203**, 1–42 (1904).

air above and below the source moves in opposite directions. Here the discontinuity in vertical velocity is proportional to a function $F(r)$ which vanishes everywhere except at $r=0$ where it becomes infinite in such a manner that its integral over the plane $z=d$ is finite.

Typical solutions of Eq. (2) are of the form,

$$\phi_1 = A\exp(-\eta z)J_0(kr)\exp(-i\omega t), \quad z>d \qquad (5)$$

$$\phi_1' = [B\exp(\eta z)+C\exp(-\eta z)]J_0(kr)\exp(-i\omega t), \\ 0<z<d \qquad (6)$$

$$\phi_3 = E\exp(\zeta z)J_0(kr)\exp(-i\omega t). \quad z<0 \qquad (7)$$

Flexural motion of the plate is given by

$$w_2 = DJ_0(kr)\exp(-i\omega t). \qquad (8)$$

The separation constants η, ζ obtained by substituting Eqs. (5)–(7) in Eq. (2) are given by

$$\eta^2 = k^2 - \omega^2/v_1^2, \quad \zeta^2 = k^2 - \omega^2/v_3^2, \qquad (9)$$

and are defined as positive real or positive imaginary.

These solutions must satisfy two additional conditions at the plane $z=d$ where the pressure is continuous,

$$\rho_1\partial\phi_1/\partial t = \rho_1\partial\phi_1'/\partial t, \qquad (10)$$

and the vertical velocity is discontinuous,

$$\partial\phi_1/\partial z - \partial\phi_1'/\partial z = 2YJ_0(kr)\exp(-i\omega t), \qquad (11)$$

the air above and below the plane moving in opposite directions.

The expression for ϕ_1' has two arbitrary constants, but ϕ_1 and ϕ_3 have been chosen to decrease exponentially with distance from the plate, since we are particularly interested in solutions for which there is no radiation from the plate into the surrounding media.

Five simultaneous linear equations result when Eqs. (5) through (8), the solutions of Eq. (2), are substituted in Eqs. (3), (4), (10), and (11), the boundary conditions. Solving for A, B, C, D, E from these equations gives:

$$A = [-Y/\eta G(k)][g(k)\exp(-\eta d)+G(k)\exp(\eta d)], \qquad (12)$$

$$B = (-Y/\eta)[\exp(-\eta d)], \qquad (13)$$

$$C = [-Y/\eta G(k)][g(k)\exp(-\eta d)], \qquad (14)$$

$$D = [-2Y/\eta G(k)][(\rho_1/\rho_2)\eta\zeta i\omega\exp(-\eta d)], \qquad (15)$$

and

$$E = [-2Y/\eta G(k)][(\rho_1/\rho_2)\omega^2\eta\exp(-\eta d)], \qquad (16)$$

where

$$G(k) = (\rho_3/\rho_2)\omega^2\eta + \eta\zeta(H\omega^2 - H^3v_p^2k^4/12 - g\rho_3/\rho_2) \\ + (\rho_1/\rho_2)\omega^2\zeta, \qquad (17)$$

$$g(k) = (\rho_3/\rho_2)\omega^2\eta + \eta\zeta(H\omega^2 - H^3v_p^2k^4/12 - g\rho_3/\rho_2) \\ - (\rho_1/\rho_2)\omega^2\zeta. \qquad (18)$$

We now generalize the discontinuity of vertical velocity in the plane $z=d$ by means of the fourier-bessel

integral,

$$F(r) = \int_0^\infty J_0(kr)kdk \int_0^\infty F(\lambda)J_0(k\lambda)\lambda d\lambda. \quad (19)$$

$F(\lambda)$ is chosen to vanish for all but infinitesimal values of λ in such a manner that

$$\int_0^\infty F(\lambda)2\pi\lambda d\lambda$$

has a finite constant value. Thus, taking $Y=kdk$ in the Eqs. (5) through (8) and (12) through (16) and integrating with respect to k from 0 to ∞, we obtain solutions which satisfy the appropriate conditions at $z=0$ and meet the additional requirements for a point source, namely continuity of pressure in the plane $z=d$ and continuity of vertical particle velocity everywhere in this plane except at the source $r=0$ where a discontinuity in $\partial\phi/\partial z$ exists proportional to

$$F(r) = \int_0^\infty J_0(kr)kdk,$$

which becomes infinite in such a way that its integral over the plane $z=d$ is finite.

The solution for a periodic point source is therefore

$$w_2 = -\exp(-i\omega t)\int_0^\infty J_0(kr)kdk$$
$$\times \{2(\rho_1/\rho_2)i\omega\zeta \exp(-\eta d)/G(k)\}. \quad (20)$$

Following the procedure of Lamb,[10] Sezawa,[11] and Pekeris,[12] Eq. (20) will be evaluated by integration along suitable contours in the complex plane $Z=k+im$. Let

$$E(Z) = -(\rho_1/\rho_2)(Z^2-\omega^2/v_3^2)^{\frac{1}{2}}i\omega \exp[-d(Z^2-\omega^2/v_1^2)^{\frac{1}{2}}],$$

and consider the two integrals whose sum can be used to evaluate the integral in Eq. (20),

$$\int_c H_0^1(Zr)[E(Z)/G(Z)]ZdZ, \quad (21)$$

and

$$\int_{c'} H_0^2(Zr)[E(Z)/G(Z)]ZdZ. \quad (22)$$

Integrals (21) and (22) are taken around paths C and C' in the first and fourth quadrants, respectively (Fig. 1). $G(Z)$ is obtained from Eq. (17). Integral (21) has branch points at $Z=\omega/v_1$ and $Z=\omega/v_3$ and a pole at $Z=k_n$, which is the root of $G(Z)=0$. $G(k_n)=0$ is the characteristic or frequency equation for air-coupled flexural waves on a floating ice sheet. Integral (22) has neither branch points nor poles. That the singular points lie in the first quadrant only can be demonstrated[11] by temporarily including small frictional forces in the original equations of motion. We denote by η', $\pm\zeta'$ the values assumed by η, ζ on both sides of the line $k=\omega/v_3$, and, by $\pm\eta''$, ζ'', the values on the two sides of $k=\omega/v_1$ (Fig. 1). For small values of m we can write:

$$\eta' = i(\omega^2/v_1^2-\omega^2/v_3^2)^{\frac{1}{2}}, \qquad \eta'' = (2m\omega/v_1)^{\frac{1}{2}}\exp(i\pi/4),$$
$$\zeta' = (2m\omega/v_3)^{\frac{1}{2}}\exp(i\pi/4), \qquad \zeta'' = (\omega^2/v_1^2-\omega^2/v_3^2)^{\frac{1}{2}}.$$

Taking integral (21) around the indicated contours and letting the radius of the circular arc approach infinity, we find

$$\int_0^\infty H_0^1(kr)[E(k)/G(k)]kdk + \int_0^\infty H_0^1(Z''r)Z''dm(\rho_1/\rho_2)\omega\zeta''$$

$$\times \left\{ \frac{\exp(-\eta''d)}{(\rho_3/\rho_2)\omega^2\eta''+\eta''\zeta''(H\omega^2-H^3v_p^2Z''^4/12-g\rho_3/\rho_2)+(\rho_1/\rho_2)\omega^2\zeta''} \right.$$

$$\left. -\frac{\exp(\eta''d)}{-(\rho_3/\rho_2)\omega^2\eta''-\eta''\zeta''(H\omega^2-H^3v_p^2Z''^4/12-g\rho_3/\rho_2)+(\rho_1/\rho_2)\omega^2\zeta''} \right\} + \int_0^\infty H_0^1(Z'r)Z'dm(\rho_1/\rho_2)\omega\exp(-\eta'd)$$

$$\times \left\{ \frac{\zeta'}{(\rho_3/\rho_2)\omega^2\eta'+\eta'\zeta'(H\omega^2-H^3v_p^2Z'^4/12-g\rho_3/\rho_2)+(\rho_1/\rho_2)\omega^2\zeta'} \right.$$

$$\left. +\frac{\zeta'}{(\rho_3/\rho_2)\omega^2\eta'-\eta'\zeta'(H\omega^2-H^3v_p^2Z'^4/12-g\rho_3/\rho_2)-(\rho_1/\rho_2)\omega^2\zeta'} \right\}$$

$$-\int_\infty^0 \frac{H_0^1(imr)mdm(\rho_1/\rho_2)\omega(m^2+\omega^2/v_3^2)^{\frac{1}{2}}\exp[-id(m^2+\omega^2/v_1^2)^{\frac{1}{2}}]}{i(\rho_3/\rho_2)\omega^2(m^2+\omega^2/v_1^2)^{\frac{1}{2}}-(m^2+\omega^2/v_1^2)^{\frac{1}{2}}(m^2+\omega^2/v_3^2)^{\frac{1}{2}}(H\omega^2-H^3v_p^2m^4/12-g\rho_3/\rho_2)+i(\rho_1/\rho_2)\omega^2(m^2+\omega^2/v_3^2)^{\frac{1}{2}}}$$

$$-2\pi i\frac{H_0^1(k_nr)k_nE(k_n)}{\partial G(k_n)/\partial k} = 0, \quad (23)$$

[11] K. Sezawa, Bull. Earth. Res. Inst. Tokyo **13**, 1, 1–17 (1935).
[12] C. L. Pekeris, Geol. Soc. Am., Mem. **27** (1948).

where k_n is the root of $G(k)=0$, $Z'=\omega/v_3+im$, and $Z''=\omega/v_1+im$, respectively, in the second and third integrals of Eq. (23). Integrating (22) around the contour in the fourth quadrant gives

$$\int_0^\infty H_0{}^2(kr)\frac{E(k)}{G(k)}kdk$$

$$-\int_{-\infty}^0 \frac{H_0{}^2(imr)mdm(\rho_1/\rho_2)\omega(m^2+\omega^2/v_3^2)^{\frac12}\exp[-id(m^2+\omega^2/v_1^2)^{\frac12}]}{i(\rho_3/\rho_2)\omega^2(m^2+\omega^2/v_1^2)^{\frac12}-(m^2+\omega^2/v_1^2)^{\frac12}(m^2+\omega^2/v_3^2)^{\frac12}(H\omega^2-H^3v_p{}^2m^4/12-g\rho_3/\rho_2)+i(\rho_1/\rho_2)\omega^2(m^2+\omega^2/v_3^2)^{\frac12}}=0.$$

$$(24)$$

The integrals along the infinite arcs in the first and fourth quadrants vanish because of the well-known properties of the hankel functions. From the relation $H_0{}^1(im)=-H_0{}^2(-im)$, it can be seen that the last integrals of Eqs. (23) and (24) are equal and opposite in sign. Since $2J_0(kr)=H_0{}^1(kr)+H_0{}^2(kr)$, the sum of the first integrals in Eqs. (23) and (24) is equivalent to Eq. (20). Using the expansions $H_0{}^1(x)\rightarrow\exp[i(x-\pi/4)]/(\pi x/2)^{\frac12}$ and $H_0{}^2(x)\rightarrow\exp[-i(x-\pi/4)]/(\pi x/2)^{\frac12}$, we add Eqs. (23) and (24) and obtain for large values of r,

$$w_2=w_0+w'+w'',$$

$$(25)$$

where w_0 represents the residue,

$$w_0=2\pi i\frac{k_n E(k_n)\exp[i(k_n r-\omega t-\pi/4)]}{(\pi k_n r/2)^{\frac12}\partial G(k_n)/\partial k},$$

$$(26)$$

and w' and w'' are the two branch line integrals,

$$w'=\frac{-2\exp[i(r\omega/v_3-\omega t-\pi/4)]}{(\pi/2)^{\frac12}}\int_0^\infty\frac{\exp(-mr)}{(Z'r)^{\frac12}}Z'dm(\rho_1/\rho_2)\omega\exp(-\eta'd)$$

$$\times\left\{\frac{(\rho_3/\rho_2)\omega^2\eta'\zeta'}{[(\rho_3/\rho_2)\omega^2\eta']^2-[\eta'\zeta'(H\omega^2-H^3v_p{}^2Z'^4/12-g\rho_3/\rho_2)+(\rho_1/\rho_2)\omega^2\zeta']^2}\right\},\quad(27)$$

$$w''=\frac{2\exp[i(r\omega/v_1-\omega t-\pi/4)]}{(\pi/2)^{\frac12}}\int_0^\infty\frac{\exp(-mr)}{(Z''r)^{\frac12}}Z''dm(\rho_1/\rho_2)\omega\zeta''$$

$$\times\left\{\frac{\cosh(\eta''d)[(\rho_3/\rho_2)\omega^2\eta''+\eta''\zeta''(H\omega^2-H^3v_p{}^2Z''^4/12-g\rho_3/\rho_2)]+\sinh(\eta''d)(\rho_1/\rho_2)\omega^2\zeta''}{-[(\rho_3/\rho_2)\omega^2\eta''+\eta''\zeta''(H\omega^2-H^3v_p{}^2k''^4/12-g\rho_3/\rho_2)]^2+[(\rho_1/\rho_2)\omega^2\zeta'']^2}\right\},\quad(28)$$

where $Z'=\omega/v_3+im$ in Eq. (27) and $Z''=\omega/v_1+im$ in Eq. (28). These definite integrals can be expanded in asymptotic forms by means of the following formula, which is readily derived from the integral representation of the gamma-function.

$$\int_0^\infty m^{\frac12}\psi(m)\exp(-mr)dm=\frac{\Gamma(3/2)}{r^{3/2}}\psi(0)+\frac{\Gamma(5/2)}{r^{5/2}}\frac{\psi'(0)}{1!}+\cdots.$$

$$(29)$$

For large r we have

$$w'\longrightarrow\frac{2i(\rho_1/\rho_3)\exp[i(r\omega/v_3-\omega t)]\exp[-id(\omega^2/v_1^2-\omega^2/v_3^2)^{\frac12}]}{r^2\omega(v_3^2/v_1^2-1)^{\frac12}},$$

$$(30)$$

$$w''\longrightarrow\frac{2\exp[i(r\omega/v_1-\omega t)]}{r^2v_1}\left\{\frac{\rho_3/\rho_1}{(\omega^2/v_1^2-\omega^2/v_3^2)^{\frac12}}+(\rho_2/\rho_1)[H-H^3v_p{}^2\omega^2/12v_1^4-g(\rho_3/\rho_2)/\omega^2]+d\right\}.$$

$$(31)$$

The solutions given by Eqs. (25) through (28) and (30) through (31) have been expressed as a residue and two integrals along branch lines. The branch line integrals represent waves which travel with velocities v_3 and v_1 and diminish rapidly for large ranges as r^{-2}. The residue represents a train of dispersive waves, whose frequency equation is given by

$$G(k_n)=0.\qquad(32)$$

Since these waves diminish in amplitude as $r^{-\frac12}$, they represent the predominant disturbance at large ranges. Using the expression for phase velocity $c=\omega/k$, we
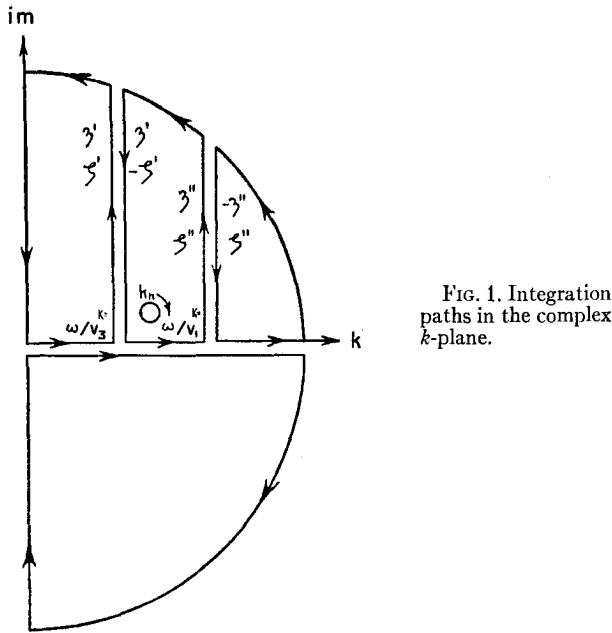
FIG. 1. Integration paths in the complex k-plane.

the dependence of amplitude upon frequency. The exponential term in Eq. (33) shows the influence of the height of the source on amplitudes. It is seen that wave amplitudes decrease exponentially as $-dk_n(1-c^2/v_1^2)^{\frac{1}{2}}$.

Generalization for an Arbitrary Pulse

In a dispersive system, such as the one under discussion, energy associated with each wavelength or frequency is known to propagate with the group velocity given by the familiar expression,

$$U = c + k dc/dk. \quad (37)$$

Carrying out the indicated differentiation, using the functional relationship between c and kH given by Eq. (36), enables one to compute values of U which are plotted in dimensionless form in Fig. 2.

Having obtained the steady-state solution for a simple harmonic point source in the air, we proceed to the case of an arbitrary initial disturbance. If the time variation of the initial disturbance at the source is $f(t)$ represented by its fourier transform,

$$g(\omega) = \int_{-\infty}^{\infty} \exp(i\omega t) f(t) dt, \quad (38)$$

then

$$f(t) = (1/2\pi) \int_{-\infty}^{\infty} \exp(-i\omega t) g(\omega) d\omega, \quad (39)$$

and the displacement w_0 becomes

$$w_0 = r^{-\frac{1}{2}} H^{-\frac{1}{2}} (2\pi v_p)^{-1} \int_{-\infty}^{\infty} g(\omega) W(k_n)$$

$$\times \exp[-dk_n(1-c^2/v_1^2)^{\frac{1}{2}}]$$

$$\times \exp[i(k_n r - \omega t - \pi/4)] d\omega. \quad (40)$$

In Eq. (40), k_n is a function of ω, through Eq. (36).

can rewrite Eq. (31) in a form more convenient for computation.

$$w_0 = \frac{W(k_n)}{r^{\frac{1}{2}} v_p H^{\frac{1}{2}}} \exp[-dk_n(1-c^2/v_1^2)^{\frac{1}{2}}]$$

$$\times \exp[i(k_n r - \omega t - \pi/4)], \quad (33)$$

where

$$W(k) = \frac{2(2\pi)^{\frac{1}{2}} (\rho_1/\rho_2)(kH)^{\frac{1}{2}} (c/v_p)(1-c^2/v_3^2)^{\frac{1}{2}}}{\{ \ \}} \quad (34)$$

$$\{ \ \} = \left\{ \frac{(\rho_3/\rho_2)c^2/v_p^2}{(1-c^2/v_1^2)^{\frac{1}{2}}} + \left[\frac{(1-c^2/v_1^2)^{\frac{1}{2}}}{(1-c^2/v_3^2)^{\frac{1}{2}}} + \frac{(1-c^2/v_3^2)^{\frac{1}{2}}}{(1-c^2/v_1^2)^{\frac{1}{2}}} \right] \right.$$

$$\times [kHc^2/v_p^2 - (kH)^3/12 - (\rho_3/\rho_2)(g/k)/v_p^2]$$

$$- (1-c^2/v_1^2)^{\frac{1}{2}}(1-c^2/v_3^2)^{\frac{1}{2}}(kH)^3/3$$

$$\left. + \frac{(\rho_1/\rho_2)c^2/v_p^2}{(1-c^2/v_3^2)^{\frac{1}{2}}} \right\}. \quad (35)$$

Equation (32) likewise may be rewritten as

$$(\rho_3/\rho_2)(c^2/v_p^2)(1-c^2/v_1^2)^{\frac{1}{2}} + (1-c^2/v_1^2)^{\frac{1}{2}}(1-c^2/v_3^2)^{\frac{1}{2}}$$
$$\times [kHc^2/v_p^2 - (kH)^3/12 - (\rho_3/\rho_2)(g/k)/v_p^2$$
$$+ (\rho_1/\rho_2)(c^2/v_p^2)(1-c^2/v_3^2)^{\frac{1}{2}} = 0. \quad (36)$$

Equation (36) is a cubic in kH with the elastic constants of the system as parameters. It defines an implicit relationship between the frequency $f = ck/2\pi$ and the phase velocity c of waves given by Eq. (32). For $c \leq v_1 < v_3$, real values of kH exist. Phase velocity in dimensionless units is plotted in Fig. 2 as a function of the dimensionless parameter $\gamma = kH/2\pi$ for the case $v_1 = 1070$ ft/sec, $v_p = 11,500$ ft/sec, $v_3 = 4650$ ft/sec, $\rho_1/\rho_2 = 0.00141$, $\rho_3/\rho_2 = 1.0904$. The factor $W(k)$ shows
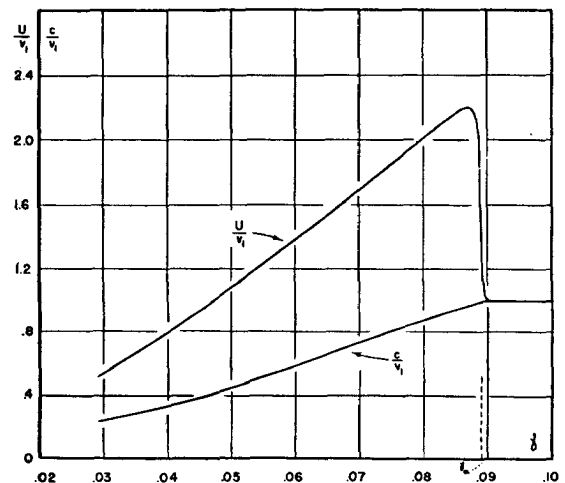

FIG. 2. Dimensionless phase velocity (c/v_1) and group velocity (U/v_1) curves.

We follow Pekeris in representing the initial disturbance created in an explosion as follows:

$$f(t) = \exp(-\sigma t) \quad t > 0 \atop = 0. \qquad t < 0 \} \qquad (41)$$

With this definition we can write

$$f(t) = (1/2\pi) \int_{-\infty}^{\infty} (\sigma - i\omega)^{-1} \exp(-i\omega t) d\omega,$$

$$g(\omega) = (\sigma - i\omega)^{-1}, \quad (42)$$

$$w_0 = r^{-\frac{1}{2}} H^{-\frac{1}{2}} (2\pi v_p)^{-1} \int_{-\infty}^{\infty} (\sigma - i\omega)^{-1} W(k_n)$$

$$\times \exp[-dk_n(1 - c^2/v_1^2)^{\frac{1}{2}}]$$

$$\times \exp[i(k_n r - \omega t - \pi/4)] d\omega. \quad (43)$$

To evaluate this integral, we use Kelvin's approximate method of stationary phase. For a discussion of this method, and the validity of the approximations used, the reader is referred to papers by Havelock,[13] Pekeris,[12] and Eckart.[14] Integrating Eq. (43) by the method of stationary phase gives

$$w_0 = \frac{W(k_0) \exp[-dk_0(1 - c^2/v_1^2)^{\frac{1}{2}}] \exp[i(k_0 r - \omega_0 t - \pi/4 \pm \pi/4)]}{rH(v_p/v_1)(\sigma - i\omega_0)[(v_1/c)(v_1/U)^2 d(U/v_1)/d\gamma]^{\frac{1}{2}}}, \qquad (44)$$

where the upper or lower sign in the exponential term is to be taken according to whether $d(U/v_1)/d\gamma$ is negative or positive; and k_0, ω_0, U/v_1, $d(U/v_1)/d\gamma$ are evaluated from the phase and group curve for values of r and t which satisfy $r/t = U$. The approximation used to derive Eq. (44) is valid provided r is large and t is sufficiently removed from stationary values of group velocity. To complete the solution we add to Eq. (44) its complex conjugate since there are two stationary points $\pm \omega_0$, and a solution to Eq. (43), except for a reversal of sign of the phase of the exponential term, would have been obtained had we assumed initially a time factor $\exp(i\omega t)$ instead of $\exp(-i\omega t)$. Thus we obtain

$$w_0 = \frac{2W(k_0) \exp[-dk_0(1 - c^2/v_1^2)^{\frac{1}{2}}] \cos(k_0 r - \omega t + \tan^{-1} \omega/\sigma)}{rH(v_p/v_1)(\sigma^2 + \omega^2)^{\frac{1}{2}}[(v_1/c)(v_1/U)^2 d(U/v_1)/d\gamma]^{\frac{1}{2}}} \qquad (45)$$

for $d(U/v_1)/d\gamma < 0$;

$$w_0 = \frac{2W(k_0) \exp[-dk_0(1 - c^2/v_1^2)^{\frac{1}{2}}] \sin(k_0 r - \omega t + \tan^{-1} \omega/\sigma)}{rH(v_p/v_1)(\sigma^2 + \omega^2)^{\frac{1}{2}}[(v_1/c)(v_1/U)^2 d(U/v_1)/d\gamma]^{\frac{1}{2}}} \qquad (46)$$

for $d(U/v_1)d\gamma > 0$.

A glance at the phase and group velocity curve in Fig. 2 shows that the approximation used in evaluating Eq. (43) fails at the times $t_m = r/U_{max}$ and $t = r/v_1$, corresponding, respectively, to the arrival of waves travelling with a maximum value of group velocity and waves for which $\gamma > \gamma_a$, where the phase and group velocity are constant.

For the maximum value of group velocity, the method of stationary phase can still be used to evaluate Eq. (43) and gives (see Havelock[13]),

$$w_0 = \frac{(4/3) \sin(\pi/3)\Gamma(1/3)W(k_0) \exp[-dk_0(1 - c^2/v_1^2)^{\frac{1}{2}}] \cos(k_0 r - \omega_0 t - \pi/4 + \tan^{-1} \omega/\sigma)}{r^{5/6}(1/6)^{\frac{1}{3}}(v_p/v_1)H^{\frac{1}{3}}(\sigma^2 + \omega^2)^{\frac{1}{2}}[2\pi H^2(v_1/c)^2(v_1/U)^2 d^2(U/v_1)/d\gamma^2]^{\frac{1}{3}}}. \qquad (47)$$

In the region $\gamma_a < \gamma < \infty$ of constant phase and group velocity, the method of stationary phase fails to evaluate the integral in Eq. (43). Waves propagated at a constant value of phase and group velocity are non-dispersive, and the signal arriving at a time $t = r/v_1$ would have the analogous characteristics of a pulse transmitted through a high pass filter with a low frequency cutoff at $f_a = \gamma_a v_1/H$. However, the excitation function $W(k)$ is vanishingly small for all $f > f_a$ and has appreciable value only at $f \simeq f_a$. Consequently, the resultant signal at $t = r/v_1$ would have the characteristics of a pulse transmitted through a sharply tuned band-pass filter with peak frequency at $f = f_a$.

Discussion of Theory

In the previous section the steady-state solution, Eq. (20), was expressed as the sum of the residue of the integrand and two integrals along branch lines corresponding to branch points $k = \omega/v_1$ and $k = \omega/v_3$. The branch line integrals represent waves travelling with velocities v_3 and v_1, respectively, and diminishing in amplitude with distance as r^{-2}. The residue contributes dispersive waves which predominate at large distance since they diminish only as $r^{-\frac{1}{2}}$. Equation (31) gives the functional relationship between phase velocity and frequency which characterizes the dispersion. Phase velocity is plotted as a function of the dimensionless parameter $\gamma = kH/2\pi = Hf/c$ in Fig. 2. Wave amplitudes for the steady state depend on frequency through the factor $W(k)$ given in Eqs. (34) through (35). A graph of $W(k)$ as a function of γ is presented in Fig. 3, for a source in the air. Interchanging the subscripts 1 and 3 in

[13] T. H. Havelock, "The Propagation of Disturbances in Dispersive Media," *Cambridge Tracts in Mathematical Physics*, No. 17 (Cambridge University Press, 1914).
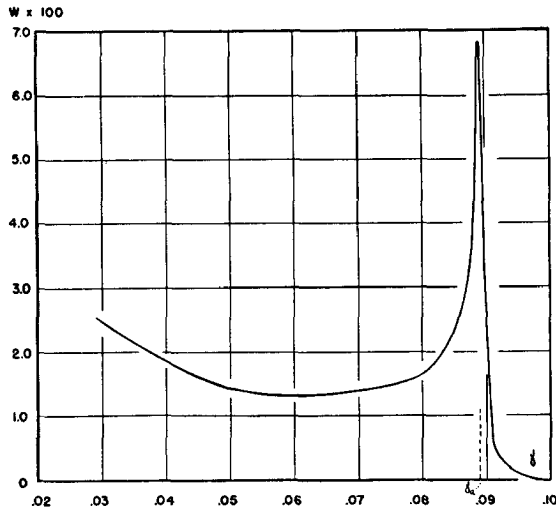[14] Carl Eckart, Revs. Modern Phys. **20**, 399–417 (1948).

FIG. 3. Steady-state amplitude function for an air source.

Eqs. (34) through (35) enables one to compute the corresponding amplitudes for a source in the water (Fig. 4).

Study of these curves for the steady state reveals that a peak amplitude exists for a point source in the air at a frequency f_a, corresponding to the phase velocity $c = v_1$. For a point source in the water, largest amplitudes are associated with low frequency waves. As the frequency (and phase velocity) increases, wave amplitudes decrease and abruptly drop to zero as the frequency f_a is approached.

Generalization of the steady-state solutions for an impulsive point source leads to the group velocity curve presented in Fig. 2. At a distant point, waves of a given frequency will arrive at a time corresponding to propagation at the group velocity associated with that frequency. In addition, wave amplitudes are proportional to the inverse square root of the slope of the group velocity curve. Referring to Eqs. (45) through (46), one
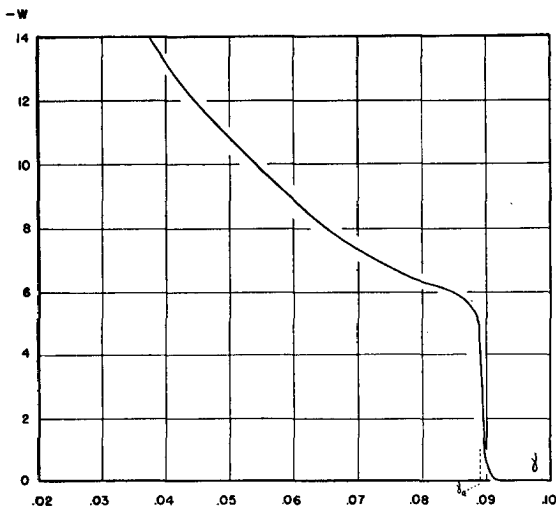

FIG. 4. Steady-state amplitude function for a water source.

can obtain an amplitude factor for an impulsive point source,

$$P(k_0) = \frac{2W(k_0) \exp[-dk_0(1-c^2/v_1^2)^{\frac{1}{2}}]}{[(v_1/c)(v_1/U)^2 d(U/v_1)/d\gamma]^{\frac{1}{2}}}, \quad (48)$$

from which wave amplitudes at large range can be obtained. Graphs of $P(k_0)$ have been computed from Eq. (48) and are presented in Figs. 5 and 6 for an air shot and water shot, respectively, located at a distance $d = 5H$ from the ice sheet. With the aid of Figs. 2, 5, and 6, one can describe, in a fairly complete manner, the sequence of waves arriving at a distant point.

For an air shot, the first waves to arrive appear at the time $t = r/2.2v_1$, corresponding to propagation at the maximum value of group velocity. These waves appear with large amplitudes and with a frequency close to f_a. As time progresses two wave trains arrive simultaneously, corresponding to the two branches of the
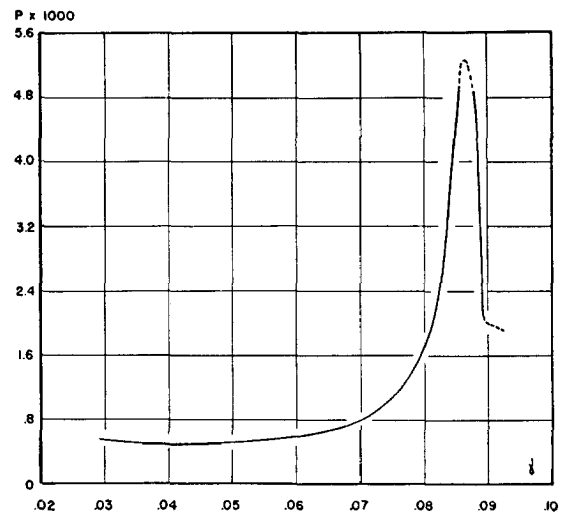
FIG. 5. Amplitude function for an air shot at $d = 5H$.

group velocity curve on either side of the maximum. Waves propagated according to the left branch of the group velocity curve are dispersive and undergo a rapid reduction in amplitude as the frequency decreases from the value f_a. Waves propagated according to the steep branch of the group velocity curve to the right of the maximum appear as a constant frequency train continuing to the time $t = r/v_1$. The constant frequency waves would appear with relatively large amplitudes since their frequency f_a is close to the peak amplitude frequency. Thus, the predominant disturbance appearing in an air shot would consist of a train of constant frequency waves beginning at the time $t = r/2.2v_1$ and ending abruptly at the time $t = r/v_1$. At this time, an air wave would arrive corresponding to the flat portion of the group velocity curve. For reasons given earlier, it would have the characteristics of a pulse transmitted through a sharply tuned band-pass filter with peak frequency at f_a.
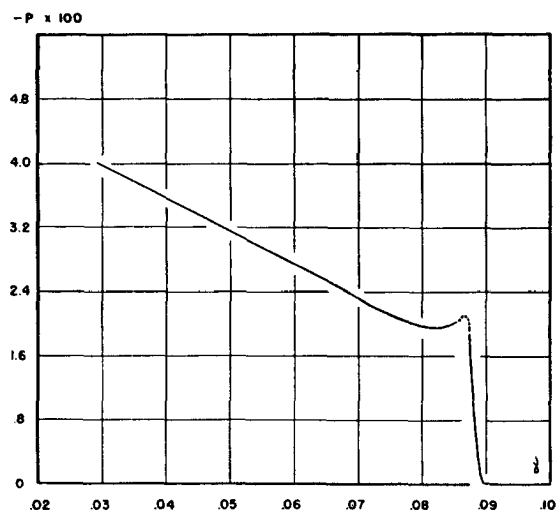
FIG. 6. Amplitude function for a water shot at $d=5H$.

FIG. 7. Observed and theoretical dispersion of flexural waves from a water shot.

For the case of a water shot the sequence of arrivals would be the same since the group velocity curve in Fig. 2 is still applicable. However, the amplitudes of the waves differ greatly (Fig. 6) in that the dispersive waves corresponding to the left branch of the group velocity curve are predominant. A water shot would therefore be characterized by a train of dispersive waves beginning at the time $t=r/2.2v_1$ with a frequency slightly less than f_a. As time increases, the frequency decreases and the amplitude increases. Although the steep portion of the group velocity curve still contributes constant frequency waves, these are now negligibly small. It is interesting to note that the portion of the group velocity curve to the left of the maximum is identical to that which would have been obtained had we neglected the air, and it is this portion of the group velocity curve which is responsible for the predominant waves appearing in a water shot. Thus, for frequencies less than f_a, the dispersion and amplitudes of flexural waves from a water shot are unaffected by the air. It is only for an air shot that a constant frequency train of "air-coupled" flexural waves appears.

Comparison with Experimental Results

Data obtained in a series of experiments on floating lake ice are in excellent agreement with the theoretical results. The standard method of seismic refraction measurements was employed in the experimental procedure. A spread consisting of 8 vertical geophones and two horizontal geophones was placed on the ice surface. Additional data were occasionally obtained from a hydrophone at various depths in the water, and a microphone in the air. Shots consisting of blasting caps or $\frac{1}{2}$ lb TNT demolition blocks detonated at various depths in the water, in the ice, and in the air. The instant of the explosion was transmitted to the recording truck by wire.

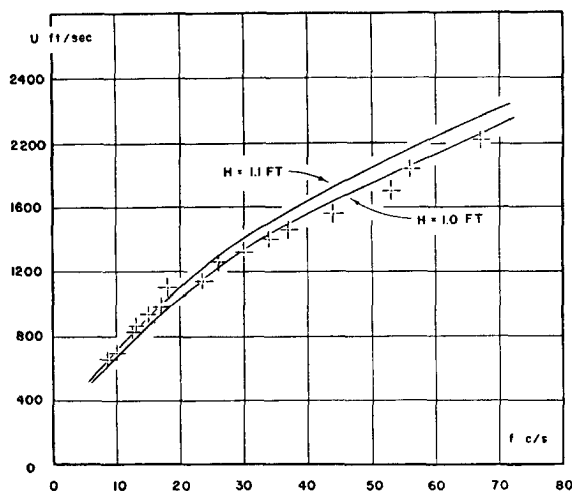Dispersion in a typical record of flexural waves for a shot consisting of a blasting cap exploded at the under surface of the ice at a spread distance of 4614–5014 ft is plotted in Fig. 7. The ice thickness averaged 12 inches and the water depth 126 ft. Good agreement with the theoretical group velocity curves for $H=1.0-1.1$ ft is found. Similar results were obtained for all shots located in the water. Dispersion was found to be independent of distance, provided shot distances were sufficiently large for the dispersion pattern to develop (>500 ft).

A pronounced change in record character was observed for shots fired on or above the ice surface. In marked contrast with the water shot, the air shot consists almost entirely of a train of constant frequency vibrations, the first wave of which travels with a velocity of about 2000 ft/sec. The constant frequency waves build up until the arrival of a pulse, after which the amplitudes diminish rapidly. The pulse consists of a single-cycle wave travelling with the speed of sound in air. Little activity can be seen in the air shot record after the arrival of the air wave, whereas in the water shot, flexural vibrations continue to arrive after the time corresponding to the air wave.

For smooth ice on Lake Superior, v_p was measured as 11,200 ft/sec, and $v_1=1070$ ft/sec. The corresponding value of γ_a is 0.091, and we can write the following simple equation for frequency of the air coupled wave in terms of ice thickness H (measured in ft):

$$f_a = \gamma_a v_1/H = 97/H. \qquad (49)$$

On the smooth ice of Lake Superior, the observed frequency f_a averaged about 78 c/s. Ice thickness sampled at 5 locations along the profile averaged 1.1 ft and the theoretically expected frequency from (49) is 88 c/s, giving reasonably good agreement in view of the uncertainty of the measured value of H.

A more detailed discussion of experimental results, in which photographs of records are presented, is in press.[8]